

AD-A285 988



ARMY RESEARCH LABORATORY



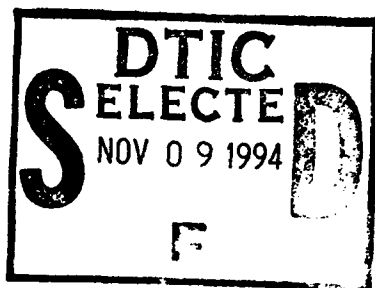
①

Quantum Chemical Study
of Rare Gas/Halide Interactions
as a Model for
High Energy Density Material:
I. Transition Properties in HC1

George F. Adams
Cary F. Chabalowski

ARL-TR-609

November 1994



278

94-34614



DTIC

APPROVED FOR PUBLIC RELEASE; DISTRIBUTION IS UNLIMITED.

94 11 7 096

NOTICES

Destroy this report when it is no longer needed. DO NOT return it to the originator.

Additional copies of this report may be obtained from the National Technical Information Service, U.S. Department of Commerce, 5285 Port Royal Road, Springfield, VA 22161.

The findings of this report are not to be construed as an official Department of the Army position, unless so designated by other authorized documents.

The use of trade names or manufacturers' names in this report does not constitute indorsement of any commercial product.

REPORT DOCUMENTATION PAGE			Form Approved OMB No. 0704-0188	
<small>Public reporting burden for this report is estimated to be 1 hour per report, including the time for reviewing instructions, searching existing data sources, gathering and maintaining the data needed, and completing and reviewing the collection of information. Send comments regarding this burden estimate or any aspect of this collection of information, including suggestions for reducing this burden, to Washington Headquarters Service, Directorate for Information Operations and Reports, U.S. Department of Commerce, Suite 1204, Washington, DC 20540-4301, and to the Office of Management and Budget, Paperwork Reduction Project (0704-0188), Washington, DC 20503.</small>				
1. AGENCY USE ONLY (Leave blank)	2. REPORT DATE November 1994	3. REPORT TYPE AND DATES COVERED Final, Sep 90 - Sep 91		
4. TITLE AND SUBTITLE Quantum Chemical Study of Rare Gas/Halide Interactions as a Model for High Energy Density Material: I. Transition Properties in HCl			5. FUNDING NUMBERS PR: 1L161102AH43	
6. AUTHOR(S) George F. Adams and Cary F. Chabalowski				
7. PERFORMING ORGANIZATION NAME(S) AND ADDRESS(ES) U.S. Army Research Laboratory ATTN: AMSRL-WT-PC Aberdeen Proving Ground, MD 21005-5066			8. PERFORMING ORGANIZATION REPORT NUMBER	
9. SPONSORING / MONITORING AGENCY NAME(S) AND ADDRESS(ES) U.S. Army Research Laboratory ATTN: AMSRL-OP-AP-L Aberdeen Proving Ground, MD 21005-5066			10. SPONSORING / MONITORING AGENCY REPORT NUMBER ARL-TR-609	
11. SUPPLEMENTARY NOTES				
12a. DISTRIBUTION / AVAILABILITY STATEMENT Approved for public release; distribution is unlimited.			12b. DISTRIBUTION CODE	
13. ABSTRACT (Maximum 200 words) <p>This is the first part of a two part study of the electronic states in a supermolecule consisting of HCl and xenon atoms, with the goal of explaining the process of transferring an electron (after photo-excitation) from a xenon atom to HCl embedded in solid xenon. The transition properties for the $\tilde{A}(1^1\Pi) \leftarrow \tilde{X}(1^1\Sigma^+)$ and $\tilde{C}(2^1\Pi) \leftarrow \tilde{X}(1^1\Sigma^+)$ transitions in HCl are studied using ab initio state averaged complete active space SCF (CASSCF) molecular orbitals plus CI. The core electrons in chlorine have been replaced with Effective Core Potentials. The photodissociation cross section $\sigma_{v=0}$ is calculated for the absorption from the $v'' = 0$ into the dissociative \tilde{A} state as a function of transition energy. The current study predicts $\sigma_{v=0}(\text{max}) = 3.9 \times 10^{-18} \text{ cm}^2$ at $\Delta E = 7.99 \text{ eV}$, in quantitative agreement with both experiment (3.8×10^{-18} at -8.0 eV), and an earlier theoretical study ($3.8 \times 10^{-18} \text{ cm}^2$ at -8.0 eV). The absorption oscillator strengths f_{0v} for the $\tilde{C} \leftarrow \tilde{X}(v=0-3)$ are also reported, with f_{00} predicted to be 0.175, in good agreement with the experimental value of 0.185 ± 0.037. The earlier theoretical study predicted $f_{00} = 0.15$, which is 19% lower than experiment. The current theoretical study differs from the previous one in our use of molecular orbitals obtained from state averaged-CASSCF, and the CI wave function expansions are approximately twice as large.</p>				
14. SUBJECT TERMS electronic states, molecular orbitals, wave functions, hydrochloric acid, photochemistry			15. NUMBER OF PAGES 24	
			16. PRICE CODE	
17. SECURITY CLASSIFICATION OF REPORT UNCLASSIFIED	18. SECURITY CLASSIFICATION OF THIS PAGE UNCLASSIFIED	19. SECURITY CLASSIFICATION OF ABSTRACT UNCLASSIFIED	20. LIMITATION OF ABSTRACT UL	

INTENTIONALLY LEFT BLANK.

TABLE OF CONTENTS

	<u>Page</u>
LIST OF FIGURES	v
LIST OF TABLES	v
1. INTRODUCTION	1
2. DETAILS OF CALCULATIONS	2
3. RESULTS	7
3.1 Properties of the $\tilde{X}(^1\Sigma^+)$, $\tilde{A}(^1\Pi)$ Electronic States	7
3.2 The $\tilde{A}(^1\Pi) \leftarrow \tilde{X}(^1\Sigma^+)$ Transition	10
3.3 The $\tilde{C}(^1\Pi) \leftarrow \tilde{X}$ Transition	15
4. DISCUSSION AND CONCLUSIONS	17
5. REFERENCES	19
DISTRIBUTION LIST	21

Accession For	
NTIS	CRA&I <input checked="" type="checkbox"/>
DTIC	TAB <input type="checkbox"/>
Unannounced	<input type="checkbox"/>
Justification	
By	
Distribution/	
Availability Codes	
Dist	Availability for Special
A-1	

INTENTIONALLY LEFT BLANK.

LIST OF FIGURES

<u>Figure</u>	<u>Page</u>
1. Potential energy curves for the $\tilde{X}(^1\Sigma^+)$ ground state, the $\tilde{A}(^1\Pi)$, and $\tilde{C}(^1\Pi)$ excited states as a function of internuclear distances in bohrs	8
2. The x-component of the electric dipole transition moment for $\tilde{A}(^1\Pi) \leftarrow \tilde{X}(^1\Sigma^+)$ as a function of internuclear distance (bohr)	12
3. The photodissociation cross section (in cm^2) as a function of ΔE for the electronic transition $\tilde{A}(^1\Pi) \leftarrow$ originating in $v'' = 0$	13
4. The photodissociation cross section (in cm^2) as a function of ΔE for the electronic transition $\tilde{A}(^1\Pi) \leftarrow \tilde{X}(^1\Sigma^+)$ originating in $v'' = 0,1,2,3$	14

LIST OF TABLES

<u>Table</u>	<u>Page</u>
1. Atomic Orbital Basis Set Used in HCl Calculations	3
2. ECP Parameters Used for Chlorine	4
3. Reference CSFs Used in the CI Procedure	6
4. Molecular Constants for the $X(^1\Sigma^+)$ and $C(^1\pi_u)$ States From This Study, Experiment, and Other Theoretical Studies	9
5. Experimental and Theoretical Electronic Transition Properties for the Single $\tilde{C} \leftarrow \tilde{X}$ and $\tilde{A} \leftarrow \tilde{X}$ Transitions	11
6. Oscillator Strengths for the $\tilde{C} \leftarrow \tilde{X}$ Transition	16

INTENTIONALLY LEFT BLANK.

1. INTRODUCTION

Fajardo and Apkarian (1986, 1988a, 1988b) have published experimental results documenting long-term energy storage (1–2 days) in solid xenon (Xe). The basic principle rests upon the formation (via laser excitation) and separation of a stable, negatively charged exciplex such as $(\text{ClXe}_2)^-$ and a self-trapped positive hole (STH) localized on a Xe_n^+ ($n = 2-3$) molecule. The first step in the formation of these separated polarons is a cooperative charge transfer excitation involving molecular Cl_2 or HCl and the Xe atoms in the solid to form



which quickly reacts with another Xe atom to form the more stable tri-atomic exciplex Xe_2^+Cl^- . This exciplex decays primarily from the $4^2\Gamma$ state through a radiative process with a natural lifetime of 225 ns (Fajardo and Apkarian 1988). The stability of the STH is related to the stabilization energy associated with crystal relaxation effects.

As an extension of our earlier studies of rare gas (Rg) atomic and molecular interactions (Chablowski et al. 1989), we begin this preliminary theoretical treatment of the Rg-halide interactions by studying the electronic states and electronic transition probabilities between electronic states in HCl . This information will be necessary to understand the results from future studies where we will explicitly include xenon atoms with the HCl , producing electronic states that are mixtures of xenon and HCl . It is also of interest to determine what effect the use of effective core potentials has on predicting known experimental molecular properties as well as properties predicted by other *ab initio* studies. Quantum chemical calculations are performed on the ground and excited states of HCl , including Effective Core Potentials (ECPs) (Wadt and Hay 1985), State Averaged-Complete Active Space MCSCF (SA-CASSCF) for generating state averaged molecular orbitals (MOs), and configuration interaction (CI) calculations to obtain the final electronic state wave functions. The primary states of interest are the ground state $\tilde{X}(^1\Sigma^+)$, and the first two excited $^1\Pi$ states, i.e., $\tilde{A}(^1\Pi)$ and $\tilde{C}(^1\Pi)$, and the electric dipole transition moments coupling the \tilde{X} with the \tilde{A} and \tilde{C} states.

There has been much previous experimental and theoretical interest in the photodissociation processes of HCl due to its important role in the chemistry of the earth's stratosphere (and that of Venus). It has also been predicted to exist in interstellar clouds in detectable amounts (Jura 1974; Dalgarno et al. 1974), but efforts to detect its emission spectra have failed in substantiating the predicted quantities (Jura and York 1978; Wright and Morton 1979). The earlier theories assumed dissociation after absorption of a

photon into only the $A(^1\Pi)$ (Roberte, Dalgarno, and Flannery 1981). The $A(^1\Pi) \leftarrow X(^1\Sigma^+)$ transition has been firmly assigned to a broad absorption band occurring at 1,400–1,800 Å. The broad nature of the band is consistent with the theoretical description (Bettendorff, Peyerimhoff, and R. J. Buenker 1982; Dishoeck, van Hemert, and Dalgarno 1982; Hirst and Guest 1980) of the upper state as being dissociative. There are reliable experimental (Inn 1975; Romand 1949; Hirst and Guest 1980) estimates of the photodissociation (absorption) cross section for the $\tilde{A} \leftarrow \tilde{X}(v'' = 0)$ band, which produces the ground electronic state atoms. (Some perturbation of this repulsive state by the xenon atoms could play an important role in the photodynamics observed for HCl in solid Xe matrices.) The first bound singlet excited state is the $\tilde{C}(^1\Pi)$, which is Rydberg in character. This is observed experimentally as an intense band system with its (0-0) vibrational band at 1,291 Å. The vibrational bands appear broadened, indicating predissociation. It has been suggested that this predissociation occurs (van Dishoeck, van Hemert, and Dalgarno 1982) by the spin-forbidden process of crossing from the singlet \tilde{C} to the repulsive $1^3\Sigma^+$ state via spin-orbit (SO) coupling(s). The potential energy curves for these two states (Bettendorff, Peyerimhoff, and Buenker 1982; van Dishoeck, van Hemert, and Dalgarno 1982) show the $1^3\Sigma^+$ crossing the \tilde{C} state near the r_e for \tilde{C} . A theoretical model for photo destruction of HCl based on the combined effects from photodissociation of \tilde{A} and the predissociation of \tilde{C} by the $1^3\Sigma^+$ state (van Dishoeck, van Hemert, and Dalgarno 1982) put the theoretical model for the photochemistry of HCl in substantially better agreement with the observed terrestrial chemistry and interstellar predictions for the abundance of HCl. Even though SO coupling could play a significant role in understanding the photo-chemical processes both in HCl and HClXe_n , we will begin by studying only the low lying singlet electronic states, with the inclusion of SO effects anticipated at the later stages in studying the HCl-Xe_n interactions.

2. DETAILS OF CALCULATIONS

The atomic orbital (AO) basis set used for H consists of four noncontracted s-type primitive Gaussians (van Duijneveldt 1971) and one p-type polarization function ($\alpha_p = 0.75$) (Frisch, Pople, and Binkley 1984), giving [4s,1p]. The Cl atom is described by a combination of ECPs and Gaussian-type orbitals (GTOs). The ECPs are those of Wadt and Hay (1985), and the GTOs consisted of three noncontracted s- and p-type valence AOs with exponents optimized for use with the ECPs (Wadt and Hay 1985). This was augmented with a negative ion function ($\alpha_p = 0.049$) and a polarization function ($\alpha_d = 0.50$) as well as a set of noncontracted Rydberg functions ($\alpha_s = 0.025$, $\alpha_p = 0.020$, $\alpha_d = 0.015$) (Dunning and Hay 1977), for a Cl basis set of [4s,5p,2d]. The H and Cl basis sets can be found in Table 1 and the ECP parameters can be found in Table 2. The CI method is the symbolic matrix element, direct CI method of Liu and Yoshimine (1981), and the SA-CASSCF procedure is the general second-order, density matrix-driven MCSCF algorithm of Lengsfeld (1982).

Table 1. Atomic Orbital Basis Set Used in HCl Calculations

Atom	Atomic Orbital	α -value	Contraction Coefficient
H ^a	s1	13.0133721	1.0
	s2	1.962496	1.0
	s3	.0444569	1.0
	s4	0.121953	1.0
	p1 ^d	0.75	1.0
Cl ^b	s1	2.231	1.0
	s2	0.472	1.0
	s3	0.1631	1.0
	s4 ^c	0.025	1.0
	p1	6.296	1.0
	p2	0.6333	1.0
	p3	0.1819	1.0
	p4 ^c	0.049	1.0
	p5 ^c	0.020	1.0
	d1 ^c	0.5	1.0
	d2 ^c	0.015	1.0

^aSee van Duijneveldt (1971).

^bSee Wadt and Hay (1985).

^cSee Dunning and Hay (1977).

^dSee Frisch, Pople, and Binkley (1984).

Table 2. ECP Parameters Used for Chlorine

Cl (ECPs) ^a	n_k	ζ_k	d_k
d potential			
	2	3.7704	-1.710217
	2	10.5841	-12.866337
	2	30.83170	-28.968595
	2	165.6440	66.272917
	1	94.8130	-10.000000
s-d potential			
	2	3.8142	35.060609
	2	18.0695	115.677712
	2	63.5622	275.672398
	1	120.3786	12.852851
	0	128.8391	3.000000
p-d potential			
	2	3.1831	15.343956
	2	13.2096	107.878824
	2	48.9869	280.800685
	2	147.4685	613.03200
	1	46.5723	7.479486
	0	216.5263	5.000000

^aSee Wadt and Hay (1985).

The $X(^1\Sigma^+)$ ground state, as well as the $\tilde{A}(^1\Pi)$ and $\tilde{C}(^1\Pi)$ excited states, are calculated over the bondlength range $R = 1.8\text{--}10.0$ bohr, at increments of 0.10 bohr between $R = 1.80\text{--}3.00$ bohr, with additional points at $R = (3.15, 3.30, 3.45, 3.60, 3.75, 3.90, 4.00, 5.00, 8.00, 10.00)$ bohr. Due to the symmetry of the molecule, only one component of each Π system need be considered and the transition properties corrected by a factor of 2 when appropriate. In the C_{2v} point group, the ground state $\tilde{X}(^1\Sigma^+)$ belongs to the A_1 irreducible representation (IRREP), while the Π_x component of the $\tilde{A}(^1\Pi)$ and $\tilde{C}(^1\Pi)$ states belongs to the B_1 IRREP. The number of active MOs used in the SA-CASSCF in each IRREP are $A_1 = 4$, $B_1 = 1$, $B_2 = 1$, $A_2 = 0$, with no frozen core orbitals outside of the implicit "frozen core" due to the ECPs. The number of active electrons per IRREP are (2,1,1,0), respectively. The number of states averaged per IRREP are (2,2,2,0) with weights of $w_i = (2, 2, 1, 1, 1, 1, 1)$, respectively.

In the CI calculations, an implicit set of frozen core orbitals once again existed due to the use of ECPs, but no other MOs were explicitly frozen out of the electronic excitations, and all virtual MOs were retained. An equivalent set of frozen core orbitals consisting of $1\sigma^2$, $2\sigma^2$, $3\sigma^2$, $4\sigma^2$, $1\pi^4$ was used in earlier CI studies by both Bettendorff, Peyerimhoff, and Buenker (1982) (BPB), and van Dishoeck, van Hemert, and Dalgarno (1982) (VVD) on HCl. BPB report potential energy curves for many electronic states but not transition properties, while VVD concentrate on fewer states, but are specifically interested in the electronic transitions between these states. In the present study, the A_1 space contains three reference configurations, including the closed shell ground state and two excited state configuration state functions (CSFs) represented by the electronic excitations $\sigma \rightarrow \sigma^*$. The 2 B_1 reference CSFs represent $\pi \rightarrow \sigma^*$ electronic excitations. Starting with the reference CSFs given in Table 3 for the A_1 and B_1 IRREPs, new CSFs are generated in a two-step process. The first step is to divide the MOs into three sets. The second step is to distribute the eight valence electrons in all symmetry-allowed combinations within these three sets, but restricting the electron occupancy in each set according to:

A_1 symmetry - Set 1 (6-4 electrons), Set 2 (0-4), Set 3 (0-2),

B_1 symmetry - Set 1 (4-2 Electrons), Set 2 (2-6), Set 3 (0-2).

This scheme for generating CSFs was chosen primarily because of its similarity to the MRD-CI²¹ scheme (excluding CSF "selection") used by VVD and BPB. The similarity may be found in the fact that this scheme generates all single and double excitations from "many" reference CSFs, these reference CSFs being generated by the electron distributions described in MO "Set 1" and "Set 2." In the MRDCI

Table 3. Reference CSFs Used in the Configuration Interaction Procedure

$\tilde{X}(^1\Sigma^+)$ (IRREP A_1)	Internal Set 1	Internal Set 2	External Set (MOs per IRREP)
	$4\sigma^2 2\pi_x^2 2\pi_y^2$	$5\sigma^2 6\sigma 7\sigma 3\pi_x 3\pi_y$	$a_1 = 5-20, b_1 = 3-8, b_2 = 3-8,$ $a_2 = 1-2$
	$4\sigma^2 2\pi_x^2 2\pi_y^2$	$5\sigma^1 6\sigma^1 7\sigma 3\pi_x 3\pi_y$	
	$4\sigma^2 2\pi_x^2 2\pi_y^2$	$5\sigma^1 6\sigma 7\sigma^1 3\pi_x 3\pi_y$	
$\tilde{A}(^1\Pi_u), C(^1\Pi_u)$ (IRREP B_1)	Internal Set 1	Internal Set 2	External Set (MOs per IRREP)
	$4\sigma^2 2\pi_y^2$	$2\pi_x^1 5\sigma^2 6\sigma^1 7\sigma 3\pi_x$	$a_1 = 16, b_1 = 6,$ $b_2 = 6, a_2 = 2$
	$4\sigma^2 2\pi_y^2$	$2\pi_x^1 5\sigma^2 6\sigma 7\sigma^1 3\pi_x$	

NOTE: See text for detailed description of internal and external MOs.

terminology, the reference CSFs given in Table 3 would best be labeled as "Main" CSFs, i.e., the largest contributors to the electronic state wave functions. This should aid in evaluating the effectiveness of the ECPs in predicting molecular properties by facilitating comparison with the widely used and well-tested *ab initio* technique employed by VVD and BPB. Table 3 also describes the MOs included in each of the three MO sets.

This scheme generated CI expansions of 7,743 and 8,434 CSFs for the A_1 and B_1 IRREPs, respectively. The lowest three roots of A_1 and B_1 symmetry were determined in the diagonalization of the CI hamiltonian matrix, but due to the choice of reference CSFs, only the $1A_1$ and $1,2B_1$ roots will be considered. The current CI expansions are larger than those used in the study by BPB, where the ground state CI wavefunction contained ~4,100 CSFs, and the excited $^1\Pi$ states had expansions around 4,400 CSFs. VVD-generated CI wavefunctions contained ~3,000 CSFs per IRREP. It must be noted that the multireference singles and doubles CI (MRD-CI) (Buenker and Peyerimhoff 1975; Bruna, Peyerimhoff, and Buenker 1980; Buenker and Phillips 1985) method used by these two previous studies contains an extrapolation technique which effectively calculates the state energies (but not the transition moments) consistent with CI expansions on the order of 71,000 CSF for the $^1\Sigma^+$ states and 64,000 CSFs for the $^1\Pi$ states in the BPB study, while VVD do not report the sizes of the CSF spaces corresponding to the extrapolated energies, but do report the use of extrapolation.

3. RESULTS

3.1 Properties of the $\tilde{X}(^1\Sigma^+)$, $\tilde{A}(^1\Pi)$, and $\tilde{C}(^1\Pi)$ Electronic States. The potential energy curves (PECs) for the three states of interest are shown in Figure 1. The molecular constants calculated from these curves are given in Table 4, along with theoretical predictions from other studies and the experimental values. The vibrational wave functions, $X_v(R)$, and frequencies are obtained from the potential energy curves for each state by solving numerically the radial Schroedinger equation for nuclear motion while ignoring rotational effects. Our results for the ground state, \tilde{X} , give $r_e = 2.43$ bohr and $\omega_e = 2,983$ cm^{-1} in good agreement with the experimental values (Huber and Herzberg 1979) of $r_e = 2.408$ bohr and $\omega_e = 2991$ cm^{-1} . The other theoretical studies listed in Table 4 also calculate these two properties to be in generally good agreement with experiment. For the $\tilde{C}(^1\Pi)$, the first bound $^1\Pi$ state, the current values for r_e and ω_e are 2.62 bohr and 2,857 cm^{-1} , respectively, while the experimental values (Tilford, Ginter, and Vanderslice 1970) are 2.55 bohr and 2,817 cm^{-1} , respectively. The theoretical work of BPB predicts $r_e = 2.60$ bohr and $\omega_e = 2,520$ cm^{-1} , and VVD predicts $r_e = 2.68$ bohr (no ω_e reported). Even though BPB's bondlength is in slightly better agreement with experiment than the current value, their ω_e differs by ~300 cm^{-1} from the current value and experiment.

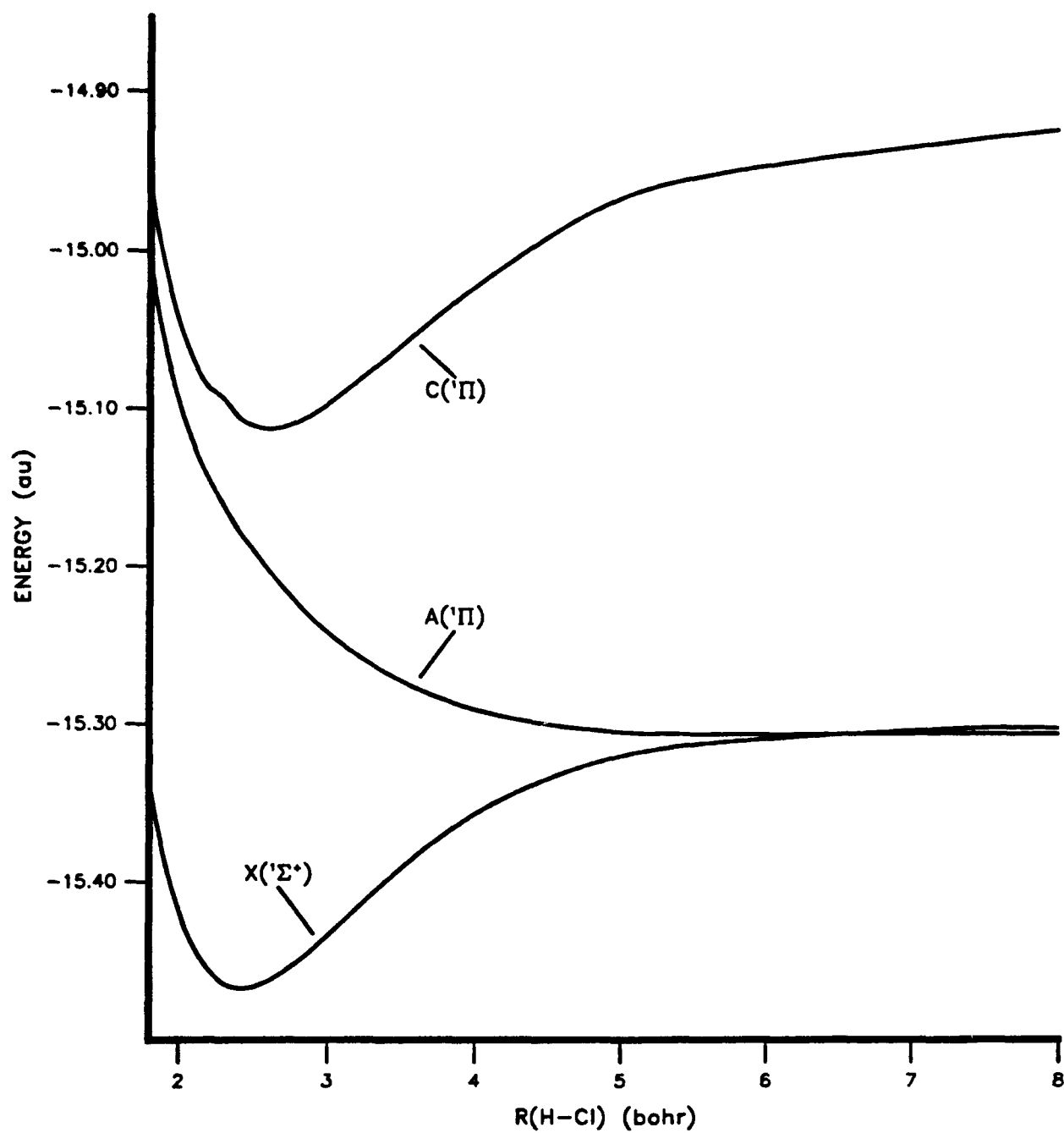


Figure 1. Potential energy curves for the $\tilde{X}(^1\Sigma^+)$ ground state, the $\tilde{A}(^1\Pi)$, and $\tilde{C}(^1\Pi)$ excited states as a function of internuclear distance in bohrs.

Table 4. Molecular Constants for the $\tilde{X}(^1\Sigma^+)$ and $\tilde{C}(^1\Pi)$ States From This Study, Experiment, and Other Theoretical Studies

	Theoretical Treatments											Experiment		
	Current Study		MRD-CI ^a		PNO-CI ^b		CEPA ^b		CI ^c					
	r_e (au)	ω_e (cm ⁻¹)	r_e	ω_e	r_e	ω_e	r_e	ω_e	r_e	ω_e	r_e	ω_e		
\tilde{X}	2.43	2,983	2.42	2,961	2.41	3,034	2.42	2,977	2.44	3,005	2.408 ^d	2,991 ^d		
\tilde{C}	2.62	2,857	2.60	2,520 not calculated								2.55 ^e	2,817 ^d
			MRD-CI ^f											
			r^e											
\tilde{X}			2.43	g										
\tilde{C}			2.68	g										

^aBettendorff, Peyerimhoff, and Buenker (1982).

^bMeyer and Rosmus (1975).

^cHirst and Guest (1980).

^dHuber and Herzberg (1979).

^eTilford, Ginter, and Vanderveke (1970).

^fvan Dishoeck, van Hemert, and Dalgaro (1982).

^gNot reported.

3.2 The $\tilde{A}(^1\Pi) \leftarrow \tilde{X}(^1\Sigma^+)$ Transition. The theoretical and experimental properties for the $\tilde{A} \leftarrow \tilde{X}$ and $\tilde{C} \leftarrow \tilde{X}$ transitions are summarized in Table 5. The X-component of the electric dipole transition moment, $\vec{\mu}_e$, versus $r_{\text{H-Cl}}$ predicted in this study, is plotted in Figure 2. As in VVD's study, our calculations show a rapidly decreasing $\vec{\mu}_e$ with increasing $r_{\text{H-Cl}}$, especially in the region near r_e . Experimentally, there is a broad absorption band with a maximum appearing near 8.0 eV, which is clearly assignable to the $\tilde{A}(^1\Pi) \leftarrow \tilde{X}(^1\Sigma^+)$ transition. The absorption represents a photodissociation cross section (van Dishoeck, van Hemert, and Dalgarno 1982), $\sigma_{v'}$, of HCl due to excitation into the repulsive \tilde{A} state (see Figure 1).

$$\sigma_{v'} = 1.225 \times 10^{-23} \cdot g \cdot \Delta E(\text{au}) \cdot |\langle \chi_k^{\tilde{A}}(R) | M \vec{\mu}_e(R) | \chi_{v'}^{\tilde{X}}(R) \rangle|^2 \text{ cm}^2 \quad (1)$$

where g is the degeneracy of the excited electronic state and $M \vec{\mu}_e$, the electronic electric dipole transition moment, is defined as

$$M \vec{\mu}_e(R) = \langle \Psi_{\tilde{A}} | \sum_i \vec{r}_i | \Psi_{\tilde{X}} \rangle. \quad (2)$$

The integral in Equation 1 is solved numerically. Figure 3 shows the results from our vibrational treatment where we predict the photodissociation cross section, $\sigma_{v'=0}$, versus ΔE . Our maximum $\sigma_{v'=0}$ value is calculated to be $3.86 \times 10^{-18} \text{ cm}^2$ at $\Delta E = 7.99 \text{ eV}$, in good agreement with the experimental value (Inn 1975) of $3.8 \times 10^{-18} \text{ cm}^2$ at $\Delta E \approx 8.0 \text{ eV}$. In the ab initio work of VVD, they calculate $\sigma_{v'=0}$ versus ΔE using both Gaussian and Slater AOs, and different sets of MOs as expansion vectors in their CIs. Their maxima (see their Figure 8) for $\sigma_{v'=0}$ also occur at $\Delta E \approx 8.0 \text{ eV}$ and range from ~ 3.6 to $\sim 4.2 \times 10^{-18} \text{ cm}^2$, giving an average of $\sim 3.9 \times 10^{-18} \text{ cm}^2$, in close agreement with both the experimental and the current value. It is interesting to note that VVD achieved good agreement with the experimental maximum for $\sigma_{v'=0}$ by averaging the results of several SCF plus CI calculations, while the present study obtained this agreement from a single set of AOs and MOs, which is most likely attributable to using MOs generated from the state averaged CASSCF procedure instead of an SCF. The photodissociation cross section for absorptions from the lowest four vibrational levels are shown in Figure 4 which again closely resemble those of VVD. The band patterns reflect the nodal structure of the vibrational wavefunctions as v'' increases from $v'' = 0 \rightarrow 3$.

Table 5. Experimental and Theoretical Electronic Transition Properties for the Single $\tilde{C} \leftarrow \tilde{X}$ and $\tilde{A} \leftarrow \tilde{X}$ Transitions

Theory					Experiment
	This Study	van Dishoeck et al ^a	Bettendorff et al ^b	Hirst and Guest ^c	
$\tilde{A}^1\Pi \leftarrow \tilde{X}^1\Sigma^+$					
$\sigma_{\nu=0}^{\max}$	$3.9 \times 10^{-18} \text{ cm}^2$ ^d	$3.7\text{-}3.8 \times 10^{-18} \text{ cm}^2$ ^e		$3.8 \times 10^{-18} \text{ cm}^2$ ^f	
ΔE_e	7.9 eV ^g	7.9 eV	7.8 eV	8.0 eV ^f	
μ_e	0.37 au at $r=2.40$	0.35-0.39 ^h at $r=2.409$	—	-----	
$\tilde{C}^1\Pi \leftarrow \tilde{X}^1\Sigma^+$					
f_{∞}	0.175	0.09-0.14 ^h		0.185 ± 0.037 ⁱ	
ΔE_{∞}	9.63 eV	not reported	9.51 eV	$(\Delta E_e) = 9.75 \text{ eV}$ 9.608 eV ^j	

^avan Dishoeck, van Hemert, and Dalgarno (1982).

^bBettendorff, Peyerimhoff, and R. J. Buenker (1982).

^cHirst and Guest (1980).

^d $\sigma_{\nu=0}^{\max}$ is maximum in the photodissociation cross section as a function of ΔE .

^e $\sigma_{\nu=0}^{\max} = 3.7\text{--}3.8 \times 10^{-18} \text{ cm}^2$, estimated from Figure 9.

^f f_{lim} (1975).

^g ΔE_e is the transition energy at maximum in $\sigma_{\nu=0}$.

^hThe range in values occur from their testing of different MOs as expansion vectors in their CIs.

ⁱSmith et al. (1980).

^jTilford, Ginter, and Vandervelde (1970).

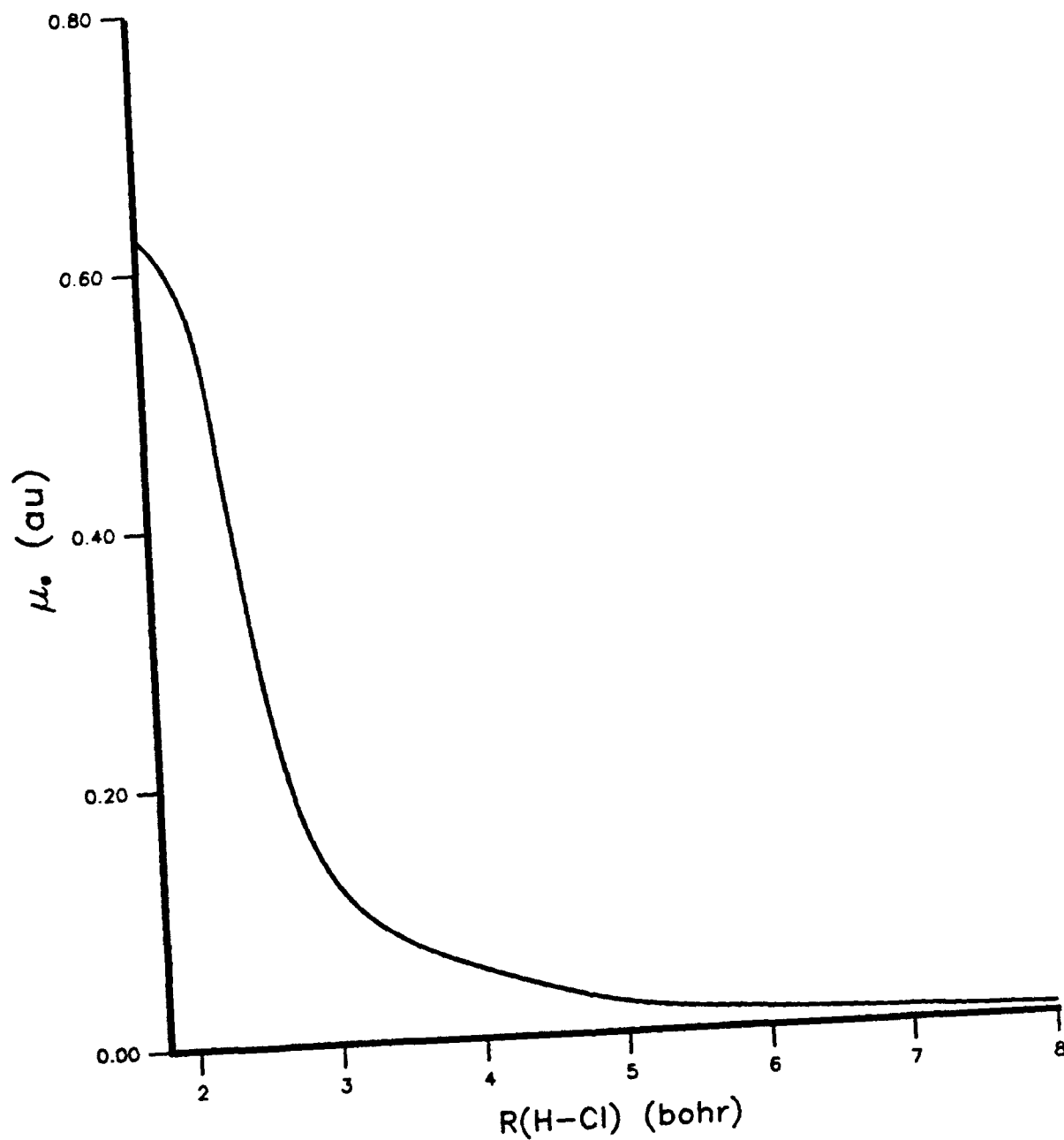


Figure 2. The x-component of the electric dipole transition moment for $\bar{A}(^1\Pi) \leftarrow \tilde{X}(^1\Sigma^+)$ as a function of internuclear distance.

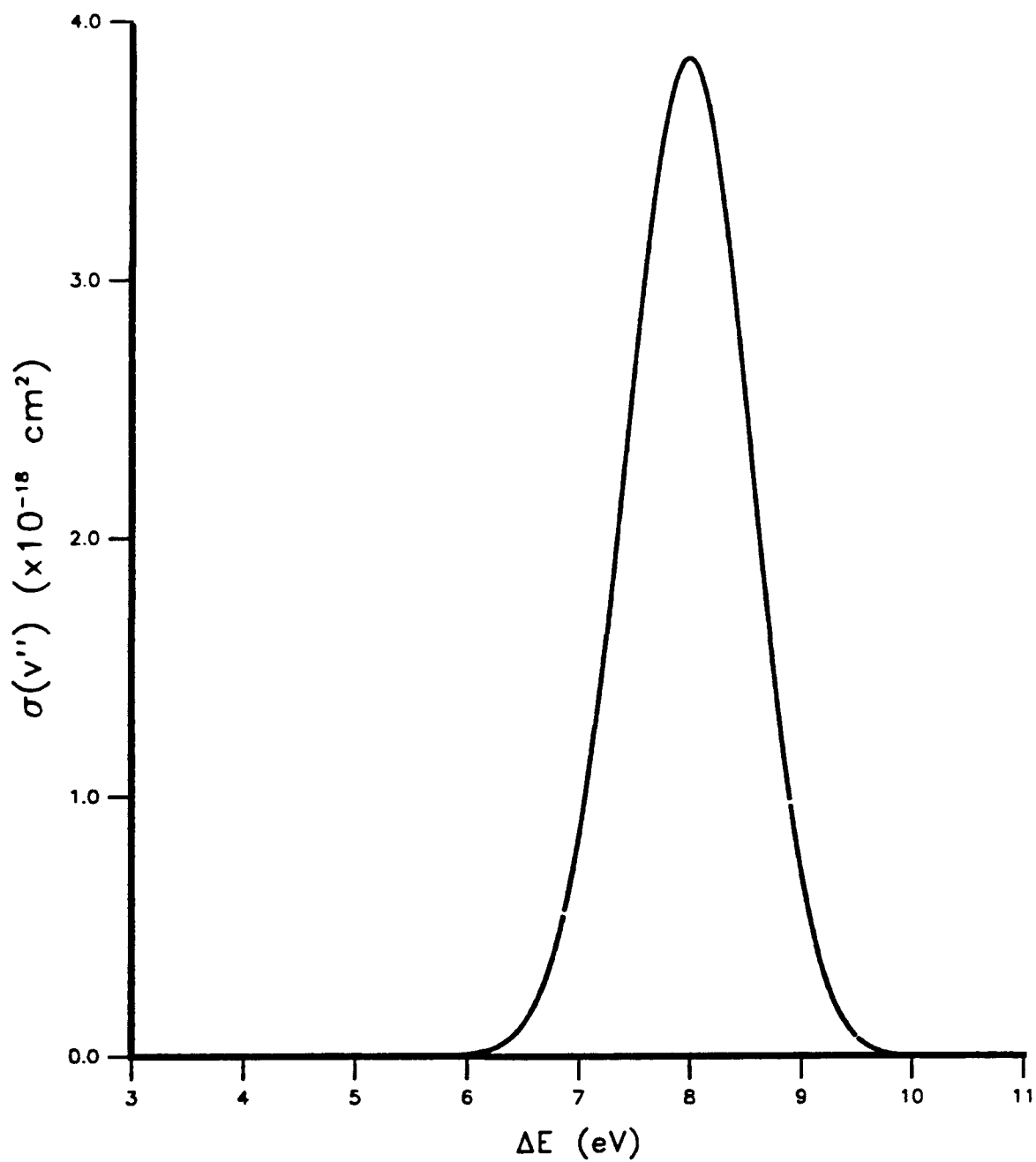


Figure 3. The photodissociation cross section (in cm²) as a function of ΔE for the electronic transition $\tilde{A}(^1\Pi) \leftarrow \tilde{X}(^1\Sigma^+)$ originating in $v'' = 0$.

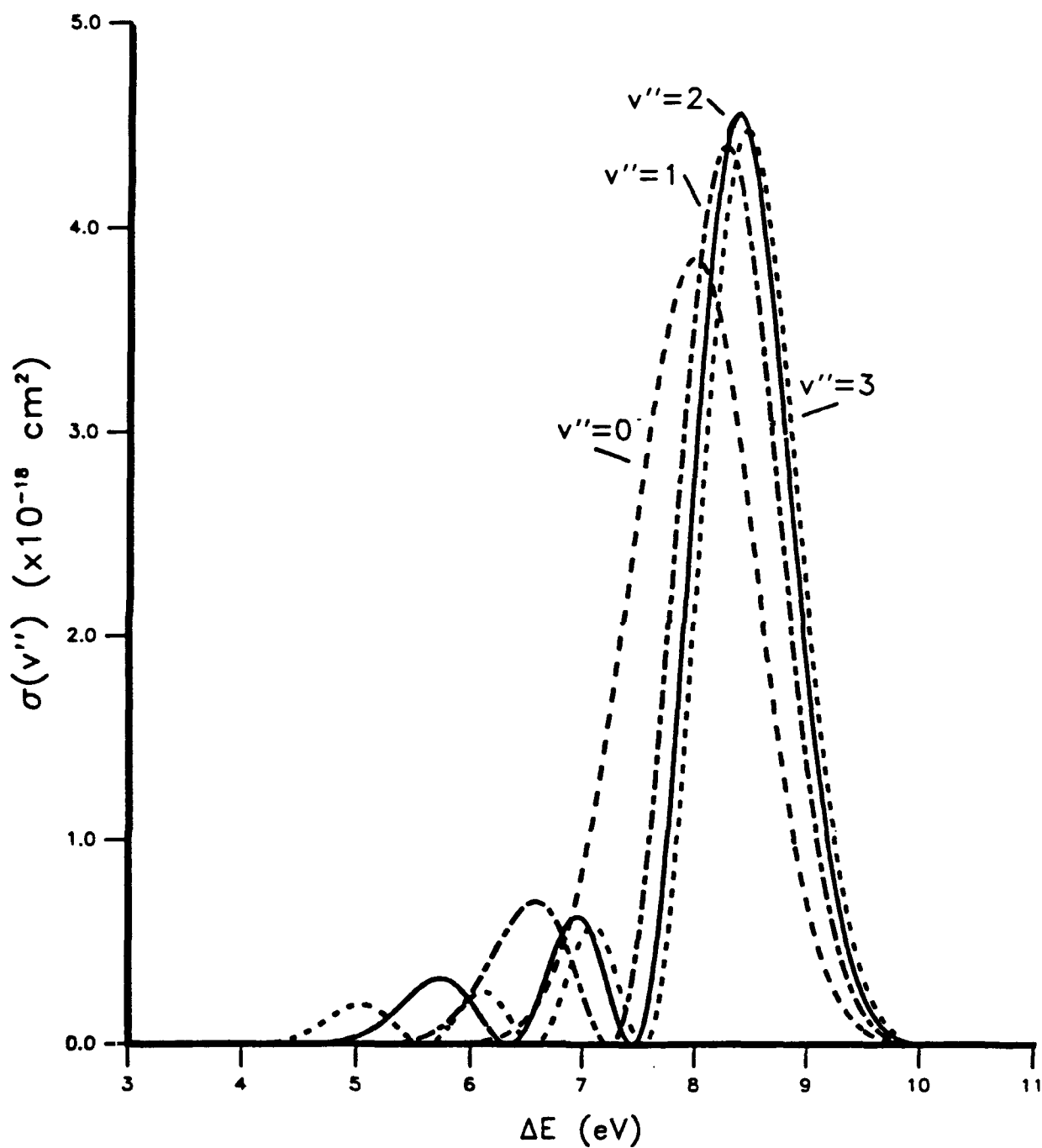


Figure 4. The photodissociation cross section (in cm^2) as a function of ΔE for the electronic transition $A(^1\Pi) \leftarrow X(^1\Sigma^+)$ originating in $v'' = 0, 1, 2, 3$.

3.3 The $\tilde{C}(^1\Pi) \leftarrow \tilde{X}(^1\Sigma)$ Transition. For the $\tilde{C}(^1\Pi) \leftarrow \tilde{X}(^1\Sigma)$ transition, experiment gives $\Delta E_{00} = 9.608$ eV, in good agreement with our value of 9.63 eV. The oscillator strength, $f_{v'-v'}$, is defined as

$$f_{v'-v'} = \frac{2}{3} g \cdot \Delta E (\text{au}) \cdot |\langle \chi_{v'}^x | \tilde{M}_e(R) | \chi_{v'}^c \rangle|^2. \quad (3)$$

The oscillator strength for the $\tilde{C} \leftarrow \tilde{X}$ 0-0 transition resulting from the vibrational analysis is $f_{00} = 0.175$, differing by 5% from the experimental value $f_{00} = 0.185 \pm 0.037$ (Smith et al. 1980; Romand 1949), and well within the experimental uncertainty. VVD calculated f_{00} using various PECs and dipole moments obtained from Gaussian and Slater AOs and using MOs optimized for different states, and found values for f_{00} ranging from $f_{00} = 0.09$ to $f_{00} = 0.14$. Their $f_{00} = 0.14$ value, which differs by 24% from experiment, came from using the all-Slater PECs and dipole moments with the $\tilde{A}(^1\Pi)$ MOs. In the all-Slater calculations, they predicted the $f_{0v'}$ values for $v' = 0-3$. And finally, they recalculated the $f_{0v'}$'s with an RKR (Ogilvie 1981) potential for the $\tilde{C}(^1\Pi)$ state, an empirical potential for the ground state, and used the dipole moments from their Slater calculations with the $\tilde{A}(^1\Pi)$ MOs. The dipole moment curve was uniformly shifted by 0.1 bohr to smaller r_{H-Cl} values because of the difference in the r_e calculated from the Slater orbitals versus the r_e predicted by the empirically fit PEC for the ground state. This approach produced a slightly larger f_{00} value of 0.15, which is 19% smaller than experiment but falls within the experimental uncertainty.

The experimental and theoretical predictions of $f_{0v'}$ for $v' = 0-3$ are collected in Table 6. The agreement between the f_{01} value from the present study and experiment is poor, with the theory predicting $f_{01} = 0.077$ and experiment giving $f_{01} = 0.022$, although the experimental value could be off by as much as a factor of two. The earlier theoretical work of van Dishoeck et al. gets $f_{01} = 0.024$ for the analysis utilizing empirically derived PECs and theoretically derived dipole moments. This value is in excellent agreement with experiment. Their $f_{0v'}$ values calculated from the all-Slater theoretical treatment are quite similar to their mixed empirical-theoretical results for $v' = 0-2$. Overall, the present study predicts the f_{00} oscillator strength in good agreement with experiment, but oscillator strengths considerably larger than experiment (or the previous theoretical study) for $v' = 1-3$. In comparison, the theoretical study of VVD calculate an oscillator strength in excellent agreement for $v' = 1$, but an f_{00} value that differs from experiment by at least 19%.

Table 6. Oscillator Strengths for the $\tilde{C} \leftarrow \tilde{X}$ Transition

v'	This Study		Experiment		van Dishoeck et al. ¹¹	
	$f_{ov'}$	$\lambda(\text{\AA})$	$f_{ov'}^a$	$\lambda(\text{\AA})^b$	All Slater ^f $f_{ov'}$	Empirical $f_{ov'}$
0	0.175	1,287	0.185 ± 0.037	1,290.6	0.14	0.15
1	0.0769	1,245	$0.022 \pm$ (factor of 2)	1,247.4	0.022 (0.02 - 0.03) ^e	0.024
2	0.0378	1,208		1,208.8	0.0028	0.0024
3	0.00722	1,176		1,174.5	0.0002	0.000006

^aSmith et al. (1980).

^bTilford, Ginter, and Vanderslice (1970).

^cThe PECs and dipole moments calculated from ab initio using Slater PECs and dipole moments.

^dOgilvie (1981).

^eFor various ab initio calculations using either gaussian or Slater PECs and dipole moments.

4. DISCUSSION AND CONCLUSIONS

The current values predicted for the \tilde{X} , \tilde{A} , and \tilde{C} state properties are seen to compare well with experiment and previous theoretical treatments of HCl. One noteworthy difference between this study and previous theoretical studies is the ω_e for the \tilde{C} state, where our value differs from experiment by 40 cm^{-1} and the best previous theoretical value by BPB differs from experiment by $\sim 300\text{ cm}^{-1}$.

With regards to the transition properties, our photodissociation cross section for the $\tilde{A} \leftarrow \tilde{X}_{v'=0}$ absorption very closely reproduces the experimental spectrum and the earlier theoretical spectrum of VVD. For the $\tilde{C} \leftarrow \tilde{X}$ transition, our $f_{00} = 0.175$ supports the higher experimental estimates of 0.185 reported by Smith et al. (1980). This casts some doubt on the lower range of values predicted by the best previous theoretical treatment where f_{00} ranges from 0.12 to 0.15 (van Dishoeck, van Hemert, and Dalgarno 1982)

The current value for f_{01} is 0.077 versus the experimental estimate 0.022 and the earlier theoretical value of 0.024. At first glance it would appear that our value for f_{01} must be in error, but the remainder of the data calculated here for the \tilde{X} and \tilde{C} states suggests otherwise. For example, our $\omega_e = 2,983\text{ cm}^{-1}$ for \tilde{X} is in excellent agreement with the experimental value of $2,991\text{ cm}^{-1}$. This suggests that the shape of our PEC for \tilde{X} near the minimum is quantitatively accurate. And for the \tilde{C} state, our ω_e is $2,857\text{ cm}^{-1}$ with experiment giving $2,817\text{ cm}^{-1}$, again in good agreement. The experiment of Tilford and Ginter (1970) predicts the energy separation between $v' = 0$ and $v' = 1$ to be $2,700\text{ cm}^{-1}$ while this study predicts $2,660\text{ cm}^{-1}$, again in excellent agreement. This would support the claim that the shape of the current PEC for the \tilde{C} state is also quantitatively accurate. Couple this information with the observation that our r_e values for both the \tilde{X} and \tilde{C} states are in good or better agreement with experiment than those from VVD, and one might conclude that our f_{00} and f_{01} values should be more accurate than those of VVD and offer quantitatively accurate values for these oscillator strengths.

The results presented in this study indicate that modest sized atomic basis sets, combined with the use of effective core potentials, MOs generated from state averaged-CASSCF, and modest sized CI wavefunctions, provide quantitative predictions for the transition properties in HCl. It should be possible to apply this level of theory to the $\text{HCl} + \text{Xe}_n$ system with the expectation of obtaining at least semi-quantitatively accurate results within the initial approximation of ignoring SO effects.

INTENTIONALLY LEFT BLANK.

5. REFERENCES

- Bettendorff, M., S. D. Peyerimhoff, and R. J. Buenker. "Clarification of the Assignment of the Electronic Spectrum of Hydrogen Chloride Based on Ab Initio Calculations." Chemical Physics, vol. 66, p. 261, 1982.
- Bruna, P. J., S. D. Peyerimhoff, and R. J. Buenker. "The Ground State of the CN^+ Ion: a Multi-Reference CI Study." Chemical Physics Letters, vol. 72, p. 278, 1980.
- Buenker, R. J., and S. D. Peyerimhoff. "Individualized Configuration Selection in CI Calculations With Subsequent Energy Extrapolation." Theoretica Chimica Acta, vol. 35, p. 33, 1974.
- Buenker, R. J., and S. D. Peyerimhoff. "Energy Extrapolation in CI Calculations." Theoretica Chimica Acta, vol. 39, p. 217, 1975.
- Buenker, R. J., and R. A. Phillips. "Implementation of the Table CI Method: Matrix Elements Between Configuration With the Same Number of Open Shells." Journal of Molecular Structure, THEOCHEM, vol. 123, p. 291, 1985.
- Chabalowski, C. F., J. O. Jensen, D. R. Yarkony, and B. H. Lengsfeld. "Theoretical Study of the Radiative Lifetime for the Spin-Forbidden Transition $a^3\Sigma_u \rightarrow X^1\Sigma_g$ in He_2 ." Journal of Chemical Physics, vol. 90, p. 2504, 1989.
- Dalgarno, A., T. de Jong, M. Oppenheimer, and J. H. Black. "Hydrogen Chloride in Dense Interstellar Clouds." Astrophysical Journal Letters, vol. 192, p. L37, 1974.
- Dunning, T. H., and P. J. Hay. Methods of Electronic Structure Theory: Modern Theoretical Chemistry, vol. 3, pp. 1-28. Edited by H. F. Schaefer III. New York: Plenum Press, 1977.
- Fajardo, M. E., and V. A. Apkarian. "Cooperative Photoabsorption Induced Charge Transfer Reaction Dynamics in Rare Gas Solids. I. Photodynamics of Localized Xenon Chloride Exciplexes." Journal of Chemical Physics, vol. 85, p. 5660, 1986.
- Fajardo, M. E., and V. A. Apkarian. "Energy Storage and Thermoluminescence in Halogen Doped Solid Xenon. III. Photodynamics of Charge Separation, Self-Trapping, and Ion-Hole Recombination." Journal of Chemical Physics, vol. 89, p. 4124, 1988a.
- Fajardo, M. E., and V. A. Apkarian. "Charge Transfer Photodynamic in Halogen Doped Xenon Matrices. II. Photoinduced Harpooning and the Delocalized Charge Transfer States of Solid Xenon Halide (F, C, B, I)." Journal of Chemical Physics, vol. 89, p. 4102, 1988b.
- Frisch, M. J., J. A. Pople, and J. S. Binkley. "Self-Consistent Molecular Orbital Methods 25. Supplementary Functions for Gaussian Basis Sets." Journal of Chemical Physics, vol. 80, p. 3265, 1984.
- Hirst, D. M., and M. F. Guest. "Excited States of HCl: an Ab Initio Configuration Interaction Investigation." Molecular Physics, vol. 41, p. 1483, 1980.
- Huber, K. P., and G. Herzberg. "Molecular Spectra and Molecular Structure." Constants of Diatomic Molecules, vol. 4, Princeton, NJ: Van Nostrand, 1979.

- Inn, E. C. Y. "Absorbion Coefficient of Hydrogen Chloride in the Region 1400 to 2200 Å." Journal of Atmospheric Science, vol. 32, p. 2375, 1975.
- Jura, M. "Chlorine Bearing Molecules in Interstellar Clouds." Astrophysical Journal Letters, vol. 190, p. L33, 1974.
- Jura, M., and D. G. York. "Observations of Interstellar Chlorine and Phosphorous." Astrophysical Journal, vol. 219, p. 861, 1978.
- Lengsfeld, B. H. "General Second-Order MCSCF Theory for Large CI Expansions." Journal of Chemical Physics, vol. 77, p. 4073, 1982.
- Liu, B., and M. Yoshimine. "The Alchemy Configuration Interaction Method. I. The Symbolic Matrix Method for Determining Elements of Matrix Operators." Journal of Chemical Physics, vol. 74, p. 612, 1981.
- Meyer, W., and P. Rosmus. "PNO-CI and CEPA Studies of Electron Correlation Effects. III. Spectroscopic Constants and Dipole Moment Functions for the Ground States of the First-Row and Second-Row Diatomic Hydrides." Journal of Chemical Physics, vol. 63, p. 2356, 1975.
- Myer, J. A., and J. A. R. Samson. "Vacuum-Ultraviolet Absorption Cross Sections of CO, HCl, and ICN Between 1050 and 2100 Å." Journal of Chemical Physics, vol. 52, p. 266, 1970.
- Ogilvie, J. F. "A General Potential Energy Function for Diatomic Molecules." Proceedings Royal Society of London, ser. a, vol. 378, p. 287, 1981.
- Roberge, W. B., A. Dalgarno, and B. P. Flannery. "Interstellar Photodissociation and Photoionization Rates." Astrophysical Journal, vol. 243, p. 817, 1981.
- Romand, J. "Ultraviolet Absorption of Gaseous HCl, HBr, and HI in the Schumann Region." Annals de Physique, vol. 4, p. 527, 1949.
- Smith, P. L., K. Yoshino, J. H. Black, and W. H. Parkinson. "Oscillator Strengths for Lines of the (0,0) and (1,0) bands of the $C^1\Pi - X^1\Sigma^+$ System of HCl and the Abundance of HCl in Diffuse Interstellar Clouds." Astrophysical Journal, vol. 238, p. 874, 1980.
- Tilford, S. G., M. L. Ginter, and T. Vanderslice. "Electronic Spectra and Structure of the Hydrogen Halide: The $b^3\Pi_1$ and $C^1\Pi$ States of HCl and DCl." Journal of Molecular Spectroscopy, vol. 33, p. 505, 1970.
- van Dishoeck, E. F., M. C. van Hemert, and A. Dalgarno. "Photodissociation Processes in the HCl Molecule." Journal of Chemical Physics, vol. 77, p. 3693, 1982.
- van Duijneveldt, F. B. IBM Research Report RJ 945, no. 16437, 10 December 1971.
- Wadt, W. R., and P. J. Hay. "Ab Initio Effective Core Potentials for Molecular Calculations. Potentials for Main Group Elements Na to Bi." Journal of Chemical Physics, vol. 82, p. 284, 1985.
- Wright, E. L., and D. C. Morton. "Rotationally Excited HD Toward Zeta OPHIUCHI." Astrophysical Journal, vol. 227, p. 483, 1979.

<u>NO. OF COPIES</u>	<u>ORGANIZATION</u>
2	ADMINISTRATOR DEFENSE TECHNICAL INFO CENTER ATTN: DTIC-DDA CAMERON STATION ALEXANDRIA VA 22304-6145
1	COMMANDER US ARMY MATERIEL COMMAND ATTN: AMCAM 5001 EISENHOWER AVE ALEXANDRIA VA 22333-0001
1	DIRECTOR US ARMY RESEARCH LABORATORY ATTN: AMSRL-OP-SD-TA/ RECORDS MANAGEMENT 2800 POWDER MILL RD ADELPHI MD 20783-1145
3	DIRECTOR US ARMY RESEARCH LABORATORY ATTN: AMSRL-OP-SD-TL/ TECHNICAL LIBRARY 2800 POWDER MILL RD ADELPHI MD 20783-1145
1	DIRECTOR US ARMY RESEARCH LABORATORY ATTN: AMSRL-OP-SD-TP/ TECH PUBLISHING BRANCH 2800 POWDER MILL RD ADELPHI MD 20783-1145
2	COMMANDER US ARMY ARDEC ATTN: SMCAR-TDC PICATINNY ARSENAL NJ 07806-5000
1	DIRECTOR BENET LABORATORIES ATTN: SMCAR-CCB-TL WATERVLIET NY 12189-4050
1	DIRECTOR US ARMY ADVANCED SYSTEMS RESEARCH AND ANALYSIS OFFICE ATTN: AMSAT-R-NR/MS 219-1 AMES RESEARCH CENTER MOFFETT FIELD CA 94035-1000

<u>NO. OF COPIES</u>	<u>ORGANIZATION</u>
1	COMMANDER US ARMY MISSILE COMMAND ATTN: AMSMI-RD-CS-R (DOC) REDSTONE ARSENAL AL 35898-5010
1	COMMANDER US ARMY TANK-AUTOMOTIVE COMMAND ATTN: AMSTA-JSK (ARMOR ENG BR) WARREN MI 48397-5000
1	DIRECTOR US ARMY TRADOC ANALYSIS COMMAND ATTN: ATRC-WSR WSMR NM 88002-5502
1	COMMANDANT US ARMY INFANTRY SCHOOL ATTN: ATSH-WCB-O FORT BENNING GA 31905-5000
	<u>ABERDEEN PROVING GROUND</u>
2	DIR, USAMSAA ATTN: AMXSY-D AMXSY-MP/H COHEN
1	CDR, USATECOM ATTN: AMSTE-TC
1	DIR, USAERDEC ATTN: SCBRD-RT
1	CDR, USACBDCOM ATTN: AMSCB-CII
1	DIR, USARL ATTN: AMSRL-SL-I
5	DIR, USARL ATTN: AMSRL-OP-AP-L

<u>NO. OF COPIES</u>	<u>ORGANIZATION</u>
1	HQDA (SARD-TR/MS K KOMINOS) WASH DC 20310-0103
1	HQDA (SARD-TR/DR R CHAIT) WASH DC 20310-0103

<u>NO. OF COPIES</u>	<u>ORGANIZATION</u>
	<u>ABERDEEN PROVING GROUND</u>
35	DIR, USARL ATTN: AMSRL-WT-P/A W HORST AMSRL-WT-PC/ R A FIFER G F ADAMS W R ANDERSON R A BEYER S W BUNTE C F CHABALOWSKI K P CLEMENTS A COHEN R CUMPTON R DANIEL D DEVYNCK N F FELL B E FORCH J M HEIMERL A J KOTLAR M R MANAA W F MCBRATNEY K L MCNESBY S V MEDLIN M S MILLER A W MIZIOLEK S H MODIANO J B MORRIS J E NEWBERRY S A NEWTON R A PESCE-RODRIGUEZ B M RICE R C SAUSA M A SCHROEDER J A VANDERHOFF M WENSING A WHREN J M WIDDER C WILLIAMSON

USER EVALUATION SHEET/CHANGE OF ADDRESS

This Laboratory undertakes a continuing effort to improve the quality of the reports it publishes. Your comments/answers to the items/questions below will aid us in our efforts.

1. ARL Report Number ARL-TR-609 Date of Report November 1994

2. Date Report Received _____

3. Does this report satisfy a need? (Comment on purpose, related project, or other area of interest for which the report will be used.) _____

4. Specifically, how is the report being used? (Information source, design data, procedure, source of ideas, etc.) _____

5. Has the information in this report led to any quantitative savings as far as man-hours or dollars saved, operating costs avoided, or efficiencies achieved, etc? If so, please elaborate. _____

6. General Comments. What do you think should be changed to improve future reports? (Indicate changes to organization, technical content, format, etc.) _____

CURRENT ADDRESS

Organization

Name

Street or P.O. Box No.

City, State, Zip Code

7. If indicating a Change of Address or Address Correction, please provide the Current or Correct address above and the Old or Incorrect address below.

OLD ADDRESS

Organization

Name

Street or P.O. Box No.

City, State, Zip Code

(Remove this sheet, fold as indicated, tape closed, and mail.)
(DO NOT STAPLE)

DEPARTMENT OF THE ARMY

OFFICIAL BUSINESS



**NO POSTAGE
NECESSARY
IF MAILED
IN THE
UNITED STATES**

BUSINESS REPLY MAIL
FIRST CLASS PERMIT NO 0001, APG, MD

Postage will be paid by addressee

Director
U.S. Army Research Laboratory
ATTN: AMSRL-OP-AP-L
Aberdeen Proving Ground, MD 21005-5066

